

Single Track of Selective Laser Melting Ti-6Al-4V Powder on Support Structure

Haijun Gong¹, Chong Teng², Kai Zeng², Deepankar Pal², Brent Stucker², J.J.S. Dilip³, Jack Beuth⁴, John J. Lewandowski⁵

¹Department of Manufacturing Engineering, Georgia Southern University, Statesboro, GA 30460

²3DSIM LLC, Park City, UT 84098

³J. B. Speed School of Engineering, University of Louisville, Louisville, KY 40292

⁴Department of Mechanical Engineering, Carnegie Mellon University, Pittsburgh, PA 15213

⁵Department of Materials Science & Engineering, Case Western Reserve University, Cleveland, OH 44106

Abstract

Melt pool shows inconsistency due to the varied heat conditions in selective laser melting (SLM) process, even if identical process parameters are used. The characterization of the actual melt pool shape is highly desired in order to eventually control the quality and property of additive manufacturing products. It has been well understood that base plate provides high thermal conduction while powder bed is low thermal condition for fusion energy to be dissipated. Based on former study of melt pool characterization on a base plate, this study creates single tracks on the support structure, which is considered the similar heat condition of the Ti-6Al-4V powder bed. Various patterns of the support structure are fabricated for single track deposition, in order to investigate the effect of the support structure on melt pool consistency and continuity. Different laser melting parameters are used in the experiments to understand their effects on the melt pool morphology.

Introduction

The advancement in solid freeform fabrication technology has attracted more and more metal parts to be produced using powder-bed-fusion based additive manufacturing processes, such as selective laser melting (SLM) and electron beam melting (EBM) [1]. The effects of EBM process parameters on material properties have been well studied with concentration on titanium alloy [2-5], while SLM provides more flexibility with various pre-alloyed powders, such as stainless steel, maraging steel, Inconel, cobalt chromium, and titanium alloys [6-10]. Many machine vendors in the U.S. market provide SLM based additive manufacturing equipment for research and industrial application. Because the SLM parts are now increasingly in use as critical components for aerospace and bio-engineering [11, 12]. The part qualification and certification are of great interest

to meet the full potential that additive manufacturing has to offer [13]. In order to well understand this powder-fusion-solid process, characterizing the foremost and basic element of SLM, i.e. single track, is highly desired to quantify its effect on the final quality of SLM products [14, 15].

Depending upon heat condition of powder bed, the melt pool of laser melting metallic powder exhibits a varied size and morphology, even if the identical scanning parameters are used. In our early study, the melt pool was characterized by creating single tracks above a base plate using Ti-6Al-4V powder [16]. The melt pool shape and size were clearly identified and recorded. It is known that the base plate provides high thermal conduction for fusion energy to be dissipated, while the powder bed may have the worst condition because thermal conductivity of gas filled pores is much lower than that of metals. Thus, to characterize the melt pool on a powder bed without any prior layers is also of great interest to researchers. However, it is hardly to fabricate and collect a consistent single track directly on the powder bed, since the molten particles accumulate to form tiny metal balls (balling effect) due to incomplete wetting [17, 18]. This explains why powder-bed-fusion based additive manufacturing process usually builds part on base plate or support structure. Hence, an investigation of single track on support structure may provide reliable information about the melt pool variation on a powder bed condition, and mimic the scenario of laser melting the first layer of powder above the support structure. In this study, Ti-6Al-4V pre-alloy powder is used for fabricating multiple support structures, followed by creating single tracks. Laser melting parameters are varied to study their influence on single track formation. The melt pool variation and the effect of support structure on single track continuity are discussed and analyzed.

Experimental Method

Ti-6Al-4V pre-alloyed powder (EOS GmbH provided) was used in an EOS M270 Direct Metal Laser Sintering (DMLS) system. The powder has an apparent density of 2.63 g/cm^3 with a mean particle size around $38 \text{ }\mu\text{m}$. The particle size has an approximate normal distribution. Most particles have a spherical or near-spherical morphology with small satellite particles attached. The EOS M270 DMLS system uses an Yb-fiber laser (max power 200W). Laser beam is guided by galvo mirrors and then focused at the powder bed. The design of support structure is customized

using Magics software. Default EOS process parameter theme is used for building support structures firstly on the base plate. Two sets of single tracks were created on the support structure.

For the first set, single tracks were fabricated with different combinations of laser power and scan speed (Factorial DOE, Table 1) on the uniform support structure, as illustrated in Fig. 1. The support structure has parallel thin walls with a spacing of 0.8 mm, on which a layer of powder ($\sim 30 \mu\text{m}$) is spread. Laser scan is then conducted with its vector perpendicular to the thin walls to form single tracks. There are a total of 42 support structures and two single beads for each.

Table 1 Factors and Levels of Factorial DOE for Single Beads

Factor	Level
Laser Power (W)	50, 75, 100, 125, 150, 175, 195
Scan Speed (mm/s)	200, 400, 600, 800, 1000, 1200

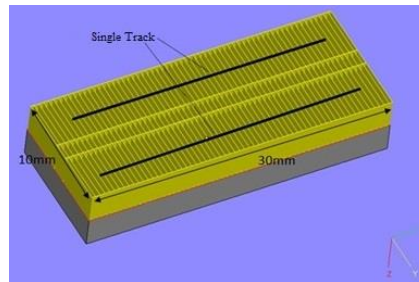


Fig. 1 schematic of single track on the uniform support structure

For the second set, four support structure patterns were utilized. As illustrated by Fig. 2, the type 1 support structure is commonly used by EOS DMLS machine for metal part fabrication. Its square mesh is oriented with certain degree. Each unit cell has a size of $0.8 \times 0.8 \text{ mm}$. The type 2 support structure has the same pattern of the type 1. But the size of unit cell is reduced to $0.6 \times 0.6 \text{ mm}$. The type 3 support structure pattern has parallel thin walls, similarly to the first set of support structures, with a reduced thin wall spacing of 0.5 mm. The type 4 support structure is re-designed based on the type 3 pattern, by adding perpendicular thin walls with a spacing of 1 mm. Single tracks are created between these thin walls, as shown in Fig. 2(d). For each pattern, 12 support structures are created to accommodate a factorial design of process parameter combinations: laser power (4 levels: 50, 100, 150, and 195 W) and scan speed (3 levels: 200, 400, and 600 mm/s). Two individual single tracks and a dual track (two adjacent single tracks) were made on each support structure. The hatch spacing of the dual track, given in Table 2, takes the size the single tracks measured from the first set for reference.

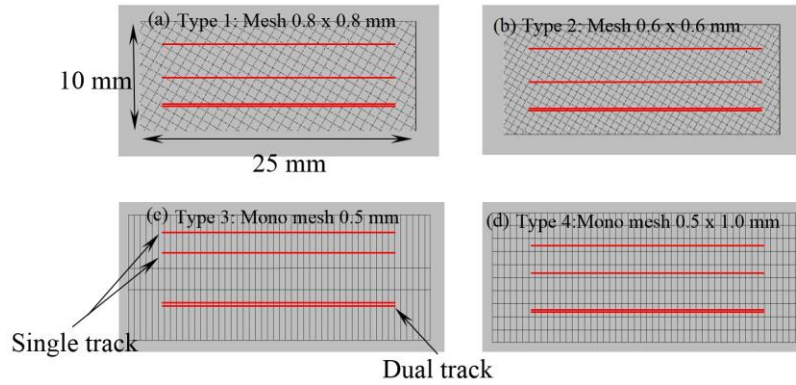


Fig. 2 schematic of single tracks on the multiple support structure patterns

Table 2 Hatch spacing of dual track (μm)

	200 mm/s	400 mm/s	600 mm/s
50 W	200	150	100
100 W	260	190	160
150 W	300	230	200
195 W	360	300	220

Results and Discussion

The effect of process parameters

Samples of single tracks on the uniform support structure (1st set) are shown in Fig. 3. The samples are equally distributed on the build plate. Each sample has two single tracks created using a unique parameter combination of laser power and scan speed.

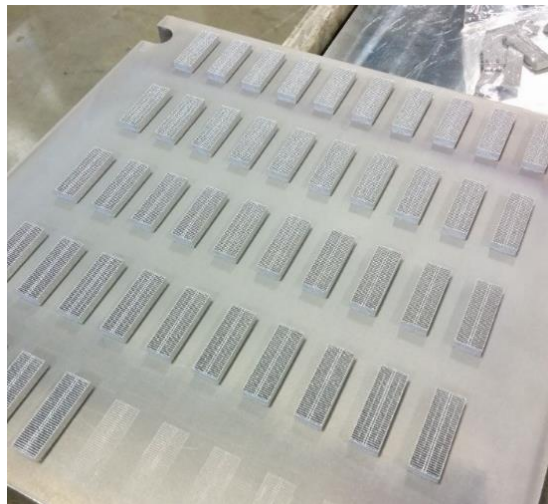


Fig. 3 samples of single track on the uniform support structure (1st set)

Micrographs of the first set of single tracks are shown in Fig. 4. The support structure has thin walls paralleled with each other, with a thickness of ~ 0.2 mm. It is noted that no continuous single track was formed on support structure. For some parameter combinations of low energy density (low laser power and high scan speed, such as 50W & 1200mm/s), laser energy fails to create continuous and consistent single tracks above support structure. Only a few solidified materials attach to the thin walls or nearby, which makes the measurement of scan track width hard to be conducted. For the parameter combinations of high energy density (high laser power and low scan speed, such as 195W & 200mm/s), the high radiation of laser energy causes drastic melting of powder and an extensive thermal field, i.e. a large melt pool. A large number of small particles which are at proximity of scan track were sintered to the solidified melt pool. The powder underneath can hardly sustain the weight of the melt pool. So the melt pool slightly shifts down into the gap of thin walls of support structure. This causes a significant difficulty in measuring the single track width, and uncertainty in estimating melt pool size.

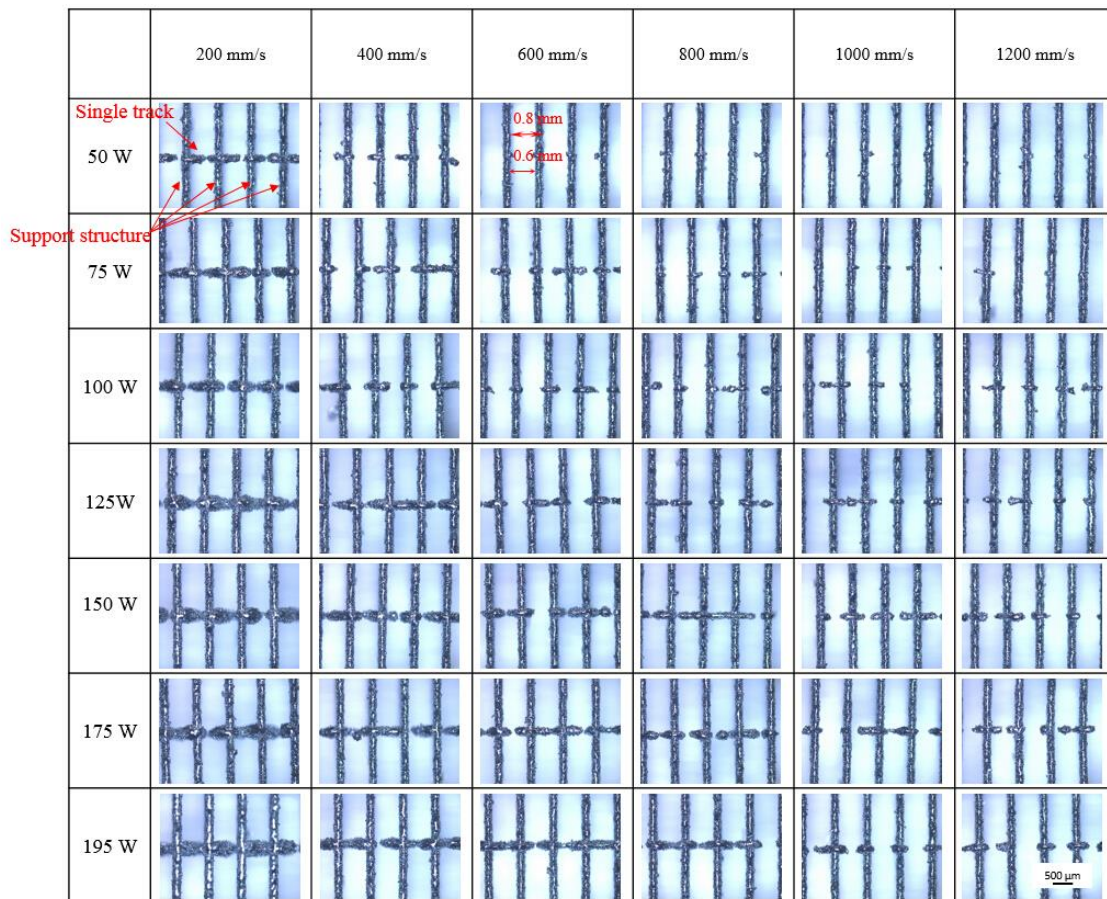


Fig. 4 microscopy of the 1st set of single tracks

The consistency and continuity of single track are attributed to many factors, such as laser energy density, powder particle distribution [19, 20], melt pool dynamics [21], or surface tension of molten material. Due to the multiple scattering, laser absorption by metal powders is significantly larger than the solid material [22]. For the low energy density parameters, a continuous melt pool is hard to be formed. Wetting of molten materials only takes place above the thin walls. Partially melted particles are removed with unmelted powder while taking the samples out of the machine. In the case of high energy density parameters, the thermal energy is hard to be dissipated due to the low thermal conductivity of powder particles. Therefore, melted particles easily accumulate to form a large melt pool (larger than laser spot size $\sim 100 \mu\text{m}$). Under the collective influence of gravity, surface tension, and wetting, the molten material sinks into the powder bed with a tendency of being close to the thin walls, so that the single track is easily broken up between the thin walls, like an unsupported overhang structure. Such kind of active melt pool has an important impact on the consistency and continuity of single tracks, in agreement with the simulation study by Cheng et al [23] that process parameters significantly affects melt pool evolution

The effect of support structure pattern

The second set of single tracks were created on a base plate, as shown in Fig. 5. Each type of support structure has 12 samples which were slightly sand blasted to remove the sintered particles after completion. The selection of process parameters for the second set of single tracks is narrowed, based on the preliminary results of the first set of samples.

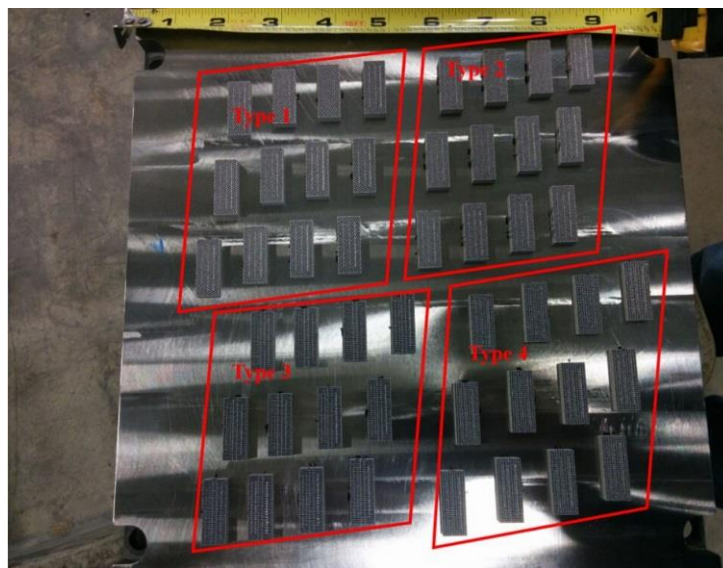


Fig. 5 samples on the multiple support structure patterns

The micrographs of single tracks on four support structure patterns are shown in Fig. 6, Fig. 7, Fig. 8, and Fig.9, respectively. The second set of support structures have a higher mesh density by adding more thin walls or reducing thin wall spacing, compared to the first set of support structure. By doing this, some process parameters are capable of generating consistent single tracks, although the scan tracks are not continuous all the way. The measurement indicates that these single tracks exhibit less variations in melt pool dimension.

The type 1 support structure is shown in Fig. 6. The thin walls have a certain angle (60°) with the single track. The distance of contacting points between the single track and thin walls is varied. Apparently, this pattern improves the continuity of the single track. It is noted that the breakpoint occurs mostly above the unsupported site (central area) of the support structure unit cell. As shown in Fig. 7, the type 2 support structure has the same pattern to type 1 support structure, but with a smaller spacing value. The reduced thin wall spacing (0.6 mm) decreases the overall distance of contacting points of single track to thin walls. So it achieves a comparable or even better continuity of single tracks on support structure. However, without supporting, the breakpoints located at some overhang sites are still hard to be eliminated along the single track.

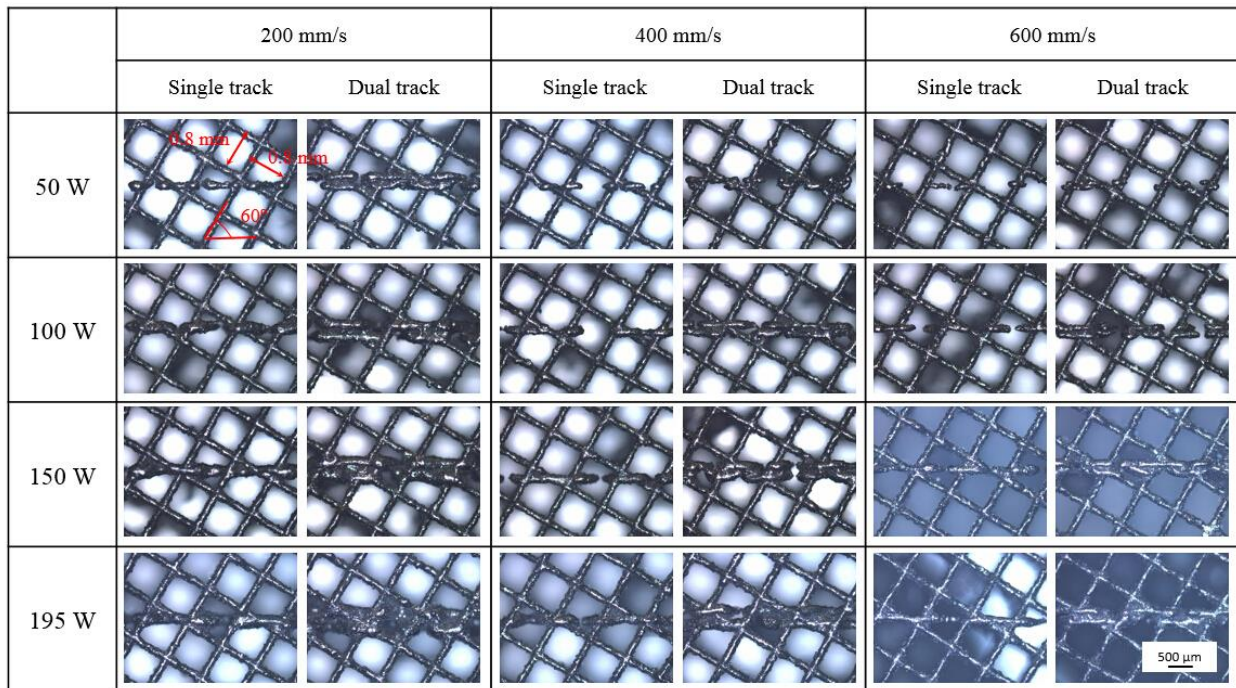


Fig. 6 single and dual tracks on type 1 support structure

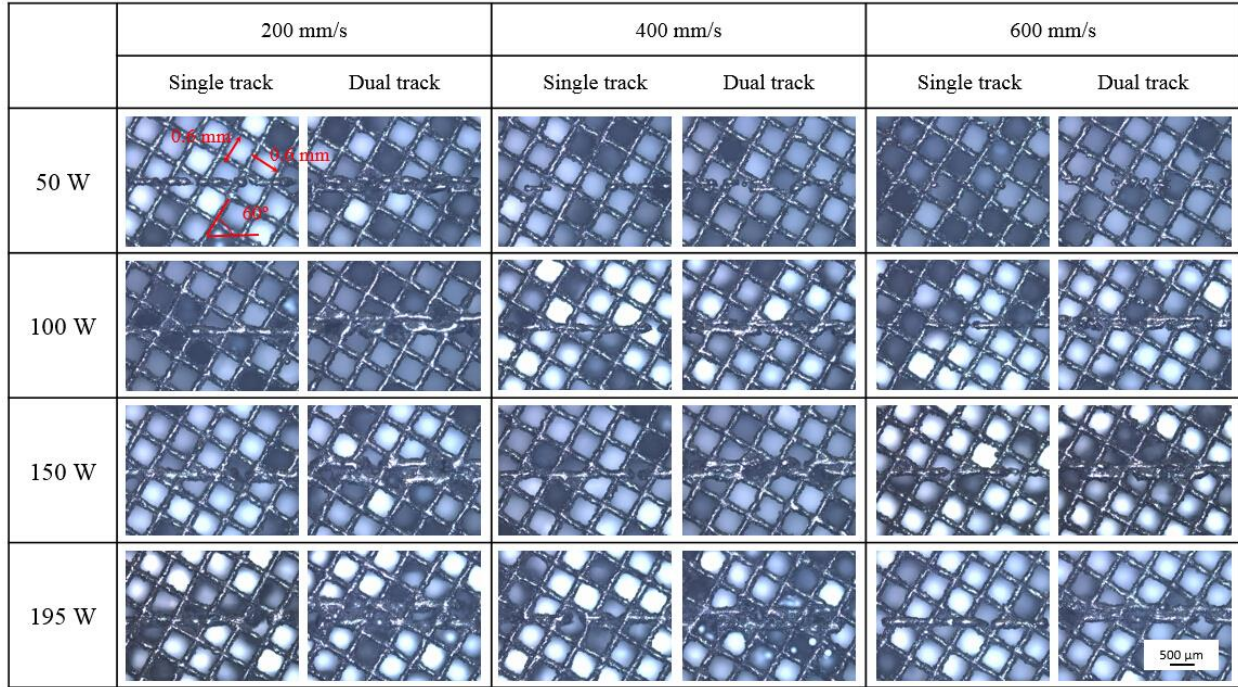


Fig. 7 single and dual tracks on type 2 support structure

The type 3 support structure pattern (Fig. 8) has the same parallel thin walls as the first set of support structures, with a reduced spacing of 0.5 mm. The single track continuity seems slightly improved, compared to Fig. 4. But it can be observed that the single track still has many breakpoints, and balling effect occurs in coincidence with some contacting points. So the consistency is not as good as the single track on the type 1 and 2 support structures, even when extra thin walls are added to the support structures (such as type 4 pattern). As shown in Fig. 9, each single track or dual track is closely surrounded by two thin walls which are oriented towards the same direction. The effective thermal conductivity was expected to be augmented to achieve a better single track continuity like type 1 and 2 support structures, since extra thin walls may help dissipate heat more quickly from the molten material. However, the observed breakpoints indicates that extra thin walls are helpless if there are no contacts with single tracks.

A measurement was performed using Olympus MX51 optical microscope to each single track at multiple locations for width dimensions. The average value of single tracks width is plotted in Fig. 10. For each single track, the standard deviation is no more than 15% of the average width. The average single track widths on type 3 and 4 support structure are slightly larger than that on type

1 and 2 support structure. This may be attributed to the difference of effective thermal conductivity of these support structures.

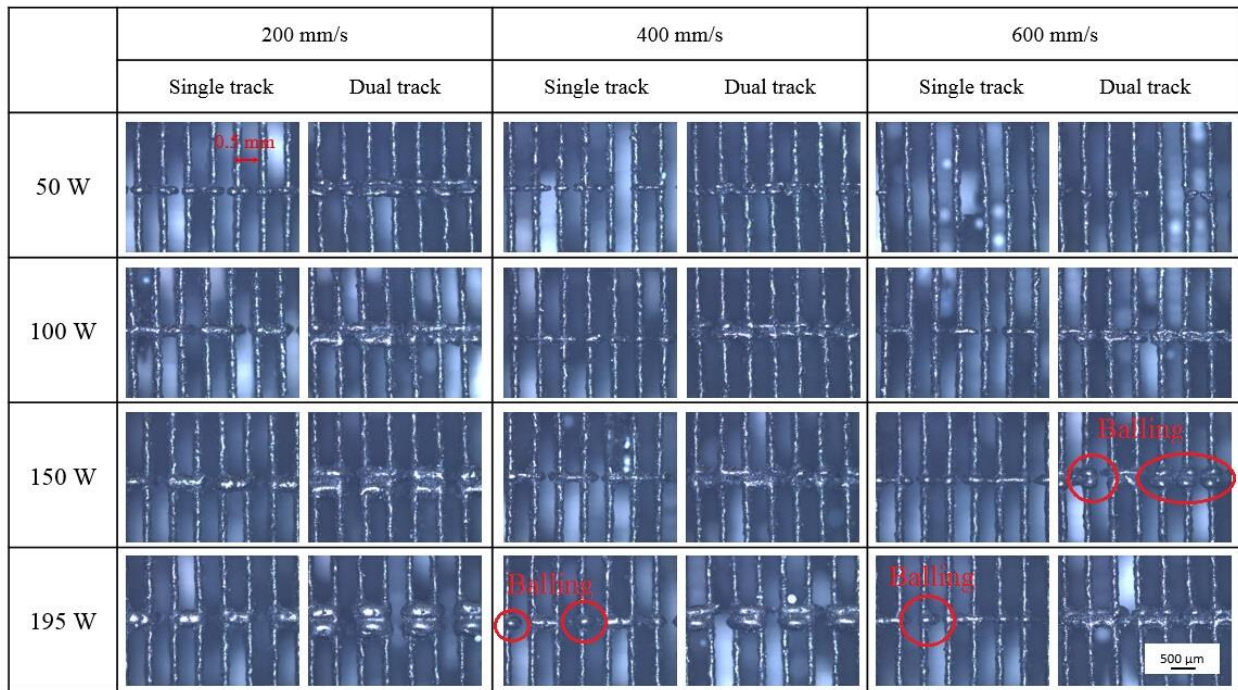


Fig. 8 single and dual tracks on type 3 support structure

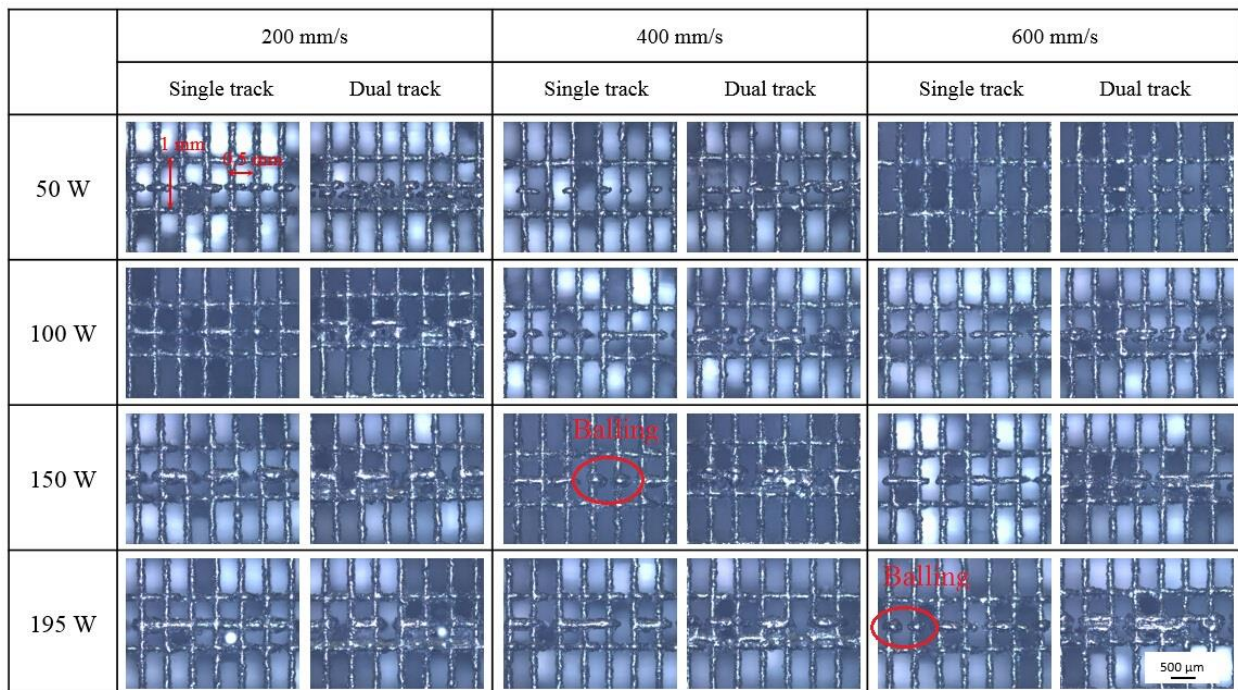


Fig. 9 single and dual tracks on type 4 support structure

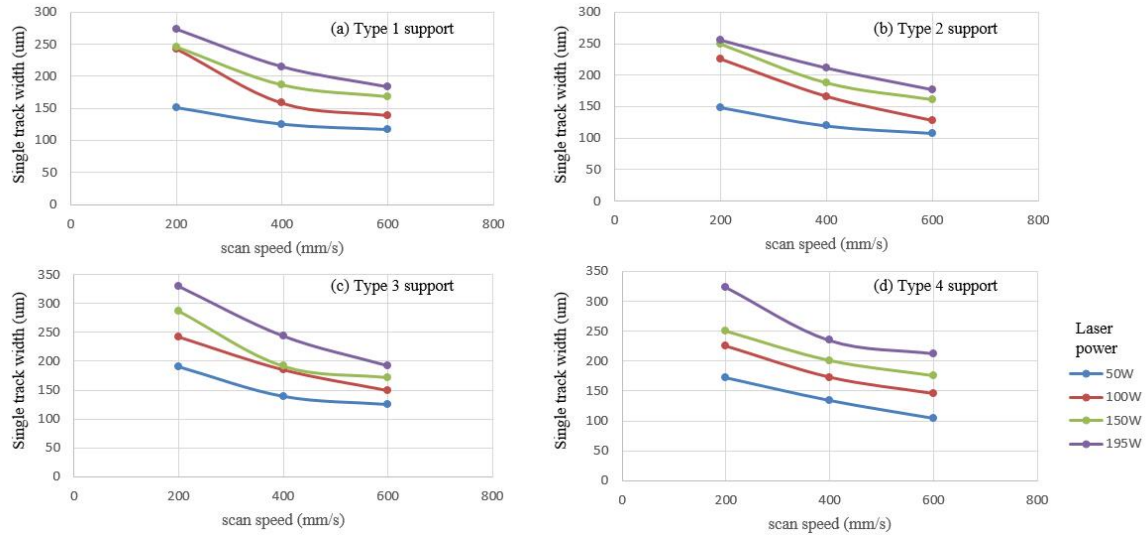


Fig. 10 Average width of single tracks on support structure

If the support structure is considered to be a cellular structure, due to geometrical regularity (in Fig. 11), its theoretical porosity (P) could be easily calculated based on the unit cell dimensions, The porosity could be thought of as an approximate indication of thermal conductivity. It makes sense that high porosity results in low thermal conductivity. Thus, a larger melt pool could be created, resulting in wider single tracks. This explains why the single track width on type 3 support structure is slightly larger than that on type 1 and 2 support structure. The effective thermal conductivity of support structure is a function of their geometry, anisotropy, and constituent independent thermal properties [24]. This suggests that the effective thermal conductivity of type 1 support structures should be higher than type 4 pattern because there are more contacts between single track and thin walls on type 1 support structure, compared to type 4 pattern. The actual thermal conduction on type 4 support structure is not as effective as type 1 support structure. So it is believed that the effective thermal conductivity of type 4 pattern should be more close to type 3 pattern.

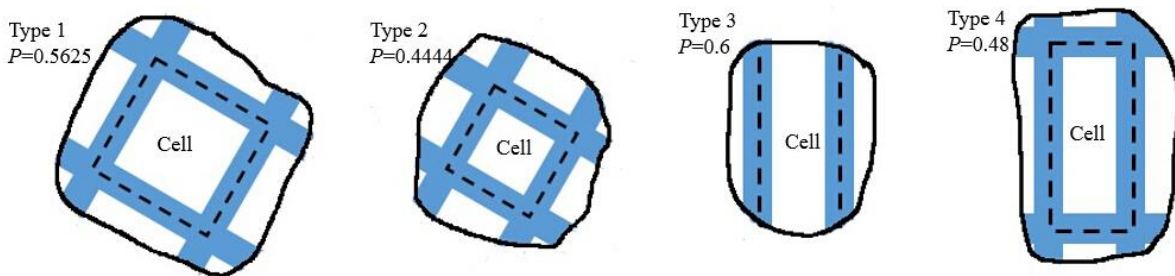


Fig. 11 unit cell and porosity of type 1-4 support structure

The effect of the continuity of prior scan tracks

Dual track reveals how the continuity is influenced by the prior scan track on the support structure. As shown in Fig. 6-9, the second single track (lower) of each dual track has the similar continuity and breakpoints, compared to the first single track (upper). This indicates that the prior scan track has a direct effect on the following scan tracks. The thin walls and prior scan tracks are the most efficient way of dissipating heat of molten material to the base plate. If powder particles are melted without contacting any support structure, the existing scan track may directly influence the thermal gradient of melt pool on a powder bed. The heat flux is somewhat oriented towards the prior scan tracks. If the thermal energy can be readily conducted away from the melt pool, molten material would be solidified continuously with a consistent morphology. Therefore, a continuous scan track is beneficial to the following scan track formation, and vice versa.

Conclusion

This experimental study provides useful information about single track formation and melt pool variation of SLM Ti-6Al-4V process. Results are also good reference for qualification and certification of other powders, and corresponding modeling and simulation research. Basically, the single track on support structure has a significant variation in continuity and consistency, in comparison with the single tracks on base plate.

Support structure is not able to provide a uniform condition for thermal conduction. Thus, significant variation of single track's dimension and discontinuity could be expected. A well-designed pattern of support structure, such as type 1 or 2 pattern, may help improve the single track's consistency and continuity. The effective thermal conductivity of support structure deserves further investigation to clarify its effects on melt pool formation. Moreover, the morphology of the prior single track has an important impact on following single tracks, as evidenced by the experimental results. Therefore, the scan strategy of the first a couple of layers needs to be carefully planned above the support structure, in order to provide a solid base for the succeeding layers.

Acknowledgement

The authors acknowledge the support of AmericaMakes through project “Rapid Qualification Methods for Powder Bed Direct Metal Additive Manufacturing Processes.” The authors also express their gratitude to the staff of the Rapid Prototyping Center at the University of Louisville for their assistance.

Reference

- [1] I. Gibson, D. Rosen, B. Stucker, Additive manufacturing technologies: rapid prototyping to direct digital manufacturing, Springer, New York, 2009.
- [2] M. Seifi, M. Dahar, R. Aman, O. Harrysson, J. Beuth, J. J. Lewandowski (2015). Evaluation of orientation dependence of fracture toughness and fatigue crack propagation behavior of as-deposited ARCAM EBM Ti-6Al-4V, *JOM*, 67(3), 597-606.
- [3] M. Seifi, I. Ghamarian, P. Samimi, U. Ackelid, P. Collins, J. J. Lewandowski (2016). Microstructure and mechanical properties of Ti-48Al-2Cr-2Nb manufactured via electron beam melting, in *Proceedings of the 13th World Conference on Titanium*, Wiley, 1317-1322.
- [4] M. Seifi, A. Salem, D. Satko, J. Shaffer, J. J. Lewandowski (2016). “Defect distribution and microstructure heterogeneity effects on fracture resistance and fatigue behavior of EBM Ti-6Al-4V”, *International Journal of Fatigue*, in press.
- [5] M. Seifi, D. Christiansen, J. Beuth, O. Harrysson, J. J. Lewandowski (2016). Process mapping, fracture and fatigue behavior of Ti-6Al-4V made by EBM additive manufacturing, in *Proceedings of the 13th World Conference on Titanium*, Wiley, 1373-1377.
- [6] H. Khalid Rafi, T. L. Starr, B. E. Stucker (2013). A comparison of the tensile, fatigue, and fracture behavior of Ti-6Al-4V and 15-5 PH stainless steel parts made by selective laser melting. *The International Journal of Advanced Manufacturing Technology*, 69(5), 1299-1309.
- [7] G. Casalino, S. L. Campanelli, N. Contuzzi, A. D. Ludovico (2015). Experimental investigation and statistical optimization of the selective laser melting process of a maraging steel. *Optics & Laser Technology*, 65, 151-158.
- [8] D. Witkin, H. Helvajian, L. Steffeney, W. Hansen (2016). Laser post-processing of Inconel 625 made by selective laser melting. *Proc. SPIE 9738, Laser 3D Manufacturing III*, 97380W.
- [9] C. Teng, H. Gong, A. Szabo, J. J. S. Dilip, K. Ashby, S. Zhang, Na. Patil, D. Pal, B. Stucker. Simulating melt pool shape and lack of fusion porosity for selective laser melting of cobalt chromium components. *Journal of Manufacturing Science and Engineering*. In print.
- [10] J.J. Lewandowski, M. Seifi (2016). Metal Additive Manufacturing: A Review of Mechanical Properties, *Annual Review of Materials Research*. 46, 151-186.
- [11] Y. van Dijk (2015). Additive manufacturing: Will it be a potential game changer for the aerospace manufacturing industry? A qualitative study of technology adoption. Master Thesis, Eindhoven University of Technology.

- [12] M. B. Bezuidenhout, D. M. Dimitrov, A. D. van Staden, G. A. Oosthuizen, L. M. T. Dicks (2015). Titanium-based hip stems with drug delivery functionality through additive manufacturing, *BioMed Research International*, Volume 2015.
- [13] M. Seifi, A. Salem, J. Beuth, O. Harrysson, J. J. Lewandowski (2016). Overview of materials qualification needs for metal additive manufacturing. *JOM*, 68(3), 747-764.
- [14] I. Yadroitsev, A. Gusarov, I. Yadroitsava and I. Smurov (2010). Single track formation in selective laser melting of metal powders. *Journal of Materials Processing Technology*, 210(12), 1624-1631.
- [15] W. King, A. T. Anderson, R. M. Ferencz, N. E. Hodge, C. Kamath, S. A. Khairallah (2015). Overview of modelling and simulation of metal powder bed fusion process at Lawrence Livermore National Laboratory, *Materials Science and Technology*, 31(8), 957-968.
- [16] H. Gong, H. Gu, K. Zeng, J.J.S. Dilip, D. Pal, B. Stucker, D. Christiansen, J. Beuth, J. J. Lewandowski (2014). Melt pool characterization for selective laser melting of Ti-6Al-4V pre-alloyed powder, *Solid Freeform Fabrication Symposium 2014*, Austin Texas.
- [17] N. K. Tolochko, S. E. Mozzharov, I. A. Yadroitsev, T. Laoui, L. Froyen, V. I. Titov, M. B. Ignatiev (2004). Balling processes during selective laser treatment of powders. *Rapid Prototyping Journal*, 10(2), 78-87.
- [18] R. Li, J. Liu, Y. Shi, L. Wang, W. Jiang (2012). Balling behavior of stainless steel and nickel powder during selective laser melting process. *The International Journal of Advanced Manufacturing Technology*, 59(9), 1025-1035.
- [19] A. B. Spierings, M. Voegtlin, T. Bauer, K. Wegener (2016). Powder flowability characterisation methodology for powder-bed-based metal additive manufacturing. *Progress in Additive Manufacturing*, 1(1), 9-20.
- [20] F. Gürtler, M. Karg, M. Dobler, S. Kohl, I. Tzivilsky, M. Schmidt (2014). Influence of powder distribution on process stability in laser beam melting: Analysis of melt pool dynamics by numerical simulations. *Solid Freeform Fabrication Symposium 2014*, Austin Texas.
- [21] T. G. Spears, S. A. Gold (2016). In-process sensing in selective laser melting (SLM) additive manufacturing. *Integrating Materials and Manufacturing Innovation*, 5:2.
- [22] C. D. Boley, S. A. Khairallah, A. M. Rubenchik (2015). Calculation of laser absorption by metal powders in additive manufacturing. *Applied Optics*, 54(9), 2477-2482.
- [23] B. Cheng, K. Chou (2015). Melt pool evolution study in selective laser melting, *Solid Freeform Fabrication Symposium 2015*, Austin Texas.
- [24] K. Zeng, D. Pal, C. Teng, B. E. Stucker (2015). Evaluations of effective thermal conductivity of support structures in selective laser melting. *Additive Manufacturing*, 6, 67-73.